

Generating single-photon catalyzed coherent states with quantum-optical catalysis

Xue-xiang Xu^{1,†} and Hong-chun Yuan²

¹College of Physics and Communication Electronics,
Jiangxi Normal University, Nanchang 330022, China

²College of Electrical and Optoelectronic Engineering,
Changzhou Institute of Technology,
Changzhou 213002, China

[†]Corresponding author: xuxuexiang@jxnu.edu.cn

We generate single-photon catalyzed coherent states (SPCCSs) by means of quantum-optical catalysis based on the beam splitter (BS) or the parametric amplifier (PA). These states are obtained in one of the BS (or PA) output channels if a coherent state and a single-photon Fock state are present in two input ports and a single photon is registered in the other output port. The success probabilities of the detection (also the normalization factors) are discussed, which is different for BS and PA catalysis. In addition, we prove that the generated states catalyzed by BS and PA devices are actually the same quantum states after analyzing photon number distribution of the SPCCSs. The quantum properties of the SPCCSs, such as sub-Poissonian distribution, anti-bunching effect, quadrature squeezing effect, and the negativity of the Wigner function are investigated in detail. The results show that the SPCCSs are non-Gaussian states with an abundance of nonclassicality, which can provide the quantum advantages for quantum technological tasks.

Keywords: beam splitter; parametric amplifier; conditional measurement; quantum-optical catalysis; non-Gaussian state; Wigner function

I. INTRODUCTION

According to von Neumann's projection principle [1], when some measurement is performed on one subsystem of the quantum-mechanically correlated system, the effect of the measurement outcome appears in the other subsystem. In particular, when a correlated two-mode optical field is prepared in an entangled state of two subsystems and the measurement is performed on one subsystem, then the quantum state of the other subsystem can be reduced to a new state [2, 3]. The unobserved output state which depends on the measurement outcome is called as the conditional output state. The measurement performed to obtain the conditional output state is named as conditional measurement. Conditional measurement may be a fruitful method for quantum-state manipulation and engineering. Many nonclassical states, such as Schrodinger-cat-like state [4], arbitrary Fock states [5], photon-subtracted traditional quantum states [6], arbitrary superposition of coherent states [7], and arbitrary multimode entangled states [8] or as well as other nonclassical states [9], have been generated by conditional measurements theoretically or experimentally.

In general, two quantum states in the two output ports of the lossless beam splitter (BS) and nondegenerate parametric amplifier (PA) are quantum-mechanically correlated with each other, even if two input states are not correlated. Hence the BS and the PA are key optical devices to obtain quantum-mechanically correlated state [10, 11]. If appropriate measurement, such as homodyne measurement and photon counting, is employed in one of the output ports, then conditional quantum state is generated in other output port. Among the schemes of conditional measurement, the most feasible strategy

is "quantum-optical catalysis", proposed by Lovvky and Mlynek [12]. They generated a coherent superposition state $t|0\rangle + \alpha|1\rangle$ by conditional measurement on a BS. This state was generated in one of the BS output channels if a coherent state $|\alpha\rangle$ and a single-photon Fock state $|1\rangle$ are present in two input ports and a single photon is registered in the other BS output. They called this transformation "quantum-optical catalysis" because the single photon itself remains unaffected but facilitate the conversion of the target ensemble. Subsequently, Bartley *et al.* [13] used "quantum-optical catalysis" to generate multiphoton nonclassical state, exhibiting a wide range of nonclassical phenomena. Recently, we operated "quantum-optical catalysis" on each mode of the two-mode squeezed vacuum state and generated a non-Gaussian two-mode quantum state with higher entanglement [14].

In 1997, Ban had derived the equivalence between BS and PA in conditional quantum measurement [15]. In other words, the conditional output of the BS is equal to that of the PA under some conditions. This inspire us to reconsider the works of Lovvky and Bartley [12]. In this work, we theoretically generate a kind of single-photon catalyzed coherent states (SPCCSs) by operating single-photon quantum-optical catalysis on a coherent state based on two kinds of quantum optical devices (BS and PA). In addition, we investigate some nonclassical properties of the generated states.

The paper is organized as follows. In Sec. II, using the BS and the PA as the basic devices we generate single-photon catalyzed coherent states (SPCCSs). The theoretical schemes are proposed and their detection probabilities are discussed. In Sec. III, we prove that the generated states by BS and PA devices are the same quantum states if the catalysis parameters are chosen appro-

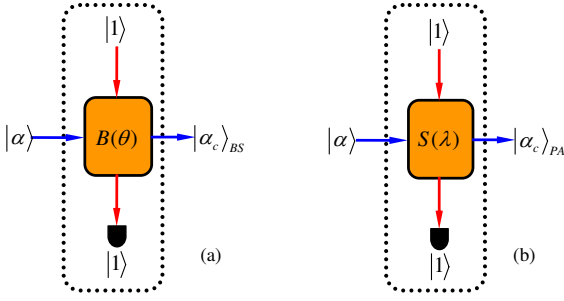


FIG. 1: (color online) Conditional generation of the SPCCSs $|\alpha_c\rangle$ with quantum-optical catalysis from a coherent state $|\alpha\rangle$, where the interaction parameter is the catalysis parameter Λ . (a) Using the BS device described with a operator $B(\theta)$ and $\Lambda = r^2 = \sin^2\theta$; (b) Using the PA device describe with a operator $S(\lambda)$ and $\Lambda = \kappa^2 = \tanh^2\lambda$. Under the constraint $\Lambda = r^2 = \kappa^2$ is satisfied, the conditional output state of the BS $|\alpha_c\rangle_{BS}$ is equal to that of the PA $|\alpha_c\rangle_{PA}$.

priately. In Sec. IV, the nonclassical properties of the generated states, such as sub-Poissonian distribution, antibunching effect, and quadrature squeezing effect are investigated. Subsequently, the negativity of the Wigner functions of the SPCCSs is investigated in Sec. V. The main results are summarized in Sec.VI.

II. SINGLE-PHOTON CATALYZED COHERENT STATE

Of all states of the radiation field, the coherent states are the most important and arise frequently in quantum optics [16]. Coherent state are generally accepted to be the most classical of the quantum states [17]. In this section, we use a coherent state (CS) as the initial state and make “quantum-optical catalysis” to induce some nonclassical states. These states will exhibit an abundance of nonclassical properties distinguished from that of the coherent states, as shown below.

As shown schematically in Fig.1, based on two kinds of optical devices (BS or PA) [18, 19], we generate the SPCCSs $|\alpha_c\rangle$ ($|\alpha_c\rangle_{BS}$ and $|\alpha_c\rangle_{PA}$). If an coherent state $|\alpha\rangle$ and a single-photon Fock state $|1\rangle$ are present in the two input ports of one optical device and a single photon $|1\rangle$ is registered in one output port, then a catalyzed state $|\alpha_c\rangle$ can be generated in the other output channel. Since the quantum-optical catalysis is a process of postselection, the success probabilities of detection are analyzed numerically.

A. SPCCS prepared by the BS device

In Fig.1(a), the role played by the lossless beam splitter (BS) upon the input state $|\psi_{in}\rangle = |\alpha\rangle_a |1\rangle_b$ results in the output state $|\psi_{out}\rangle = B(\theta) |\alpha\rangle_a |1\rangle_b$, where $B(\theta) = \exp[\theta(a^\dagger b - ab^\dagger)]$ corresponds to the unitary operator

of the adjustable BS $B(\theta)$ in terms of the creation (annihilation) operator $a^\dagger(a)$ and $b^\dagger(b)$ for modes a and b , which fulfill $Ba^\dagger B^\dagger = a^\dagger t - b^\dagger r$ and $Bb^\dagger B^\dagger = a^\dagger r + b^\dagger t$ with $r = \sin\theta$ and $t = \cos\theta$ ($\theta \in [0, \pi/2]$). After registering single-photon in the output mode b , a SPCCS is obtained in a channel

$$\begin{aligned} |\alpha_c\rangle_{BS} &= \frac{1}{\sqrt{p_{BS}}} {}_b\langle 1| B(\theta) |\alpha\rangle_a |1\rangle_b \\ &= c_0 |t\alpha\rangle + c_1 a^\dagger |t\alpha\rangle, \end{aligned} \quad (1)$$

where $|t\alpha\rangle$ is a new coherent state and $c_0 = t e^{-r^2|\alpha|^2/2}/\sqrt{p_{BS}}$, $c_1 = -r^2 \alpha e^{-r^2|\alpha|^2/2}/\sqrt{p_{BS}}$. In addition, the normalization factor $p_{BS} = e^{-r^2|\alpha|^2} I_0(\alpha, r^2)$ is the success probability heralded by the detection of a single photon at the mode, where the function $I_0(\alpha, r^2)$ is defined in appendix. Obviously, $I_0(\alpha, 0) = 1$ and $I_0(\alpha, 1) = |\alpha|^2$. The success probability p_{BS} of obtaining the SPCCSs $|\alpha_c\rangle_{BS}$ is plotted in the $(|\alpha|, r^2)$ parameter space in Fig.2 (a) and (c).

B. SPCCS prepared by the PA device

In Fig.1(b), the role played by the nondegenerate parametric amplifier (NOPA) upon the input state $|\psi_{in}\rangle = |\alpha\rangle_a |1\rangle_b$ results in the output state $|\psi_{out}\rangle = S(\lambda) |\alpha\rangle_a |1\rangle_b$, where $S(\lambda) = \exp[\lambda(a^\dagger b^\dagger - ab)]$ corresponds to the two-mode squeezed operator with real squeezing parameter λ , which fulfill $Sa^\dagger S^\dagger = \varkappa^{-1} a^\dagger - \kappa \varkappa^{-1} b$, $Sb^\dagger S^\dagger = \varkappa^{-1} b^\dagger - \kappa \varkappa^{-1} a$ with $\kappa = \tanh\lambda$ and $\varkappa = \cosh^{-1}\lambda$ ($\lambda \in [0, \infty)$). Similarly, when single-photon is detected in the b channel, a SPCCS is obtained in the a channel

$$\begin{aligned} |\alpha_c\rangle_{PA} &= \frac{1}{\sqrt{p_{PA}}} {}_b\langle 1| S(\lambda) |\alpha\rangle_a |1\rangle_b \\ &= d_0 |\varkappa\alpha\rangle + d_1 a^\dagger |\varkappa\alpha\rangle, \end{aligned} \quad (2)$$

where $|\varkappa\alpha\rangle$ is also a coherent state and $d_0 = \varkappa^2 e^{-\kappa^2|\alpha|^2/2}/\sqrt{p_{PA}}$ and $d_1 = -\varkappa \kappa^2 \alpha e^{-\kappa^2|\alpha|^2/2}/\sqrt{p_{PA}}$. In addition, the normalization factor $p_{PA} = (1 - \kappa^2) e^{-\kappa^2|\alpha|^2} I_0(\alpha, \kappa^2)$ is the success probability of such event. The success probability p_{PA} of obtaining the SPCCSs $|\alpha_c\rangle_{PA}$ are plotted in the $(|\alpha|, \kappa^2)$ parameter space in Fig.2 (b) and (d).

III. EQUIVALENT EFFECT OF BS AND PA IN PREPARING THE SPCCS

From Eqs.(1) and (2), we find that the SPCCSs ($|\alpha_c\rangle_{BS}$ and $|\alpha_c\rangle_{PA}$) are the coherent superposition state of a coherent state (Gaussian, $|t\alpha\rangle$ or $|\varkappa\alpha\rangle$) and a single-photon-added coherent state (non-Gaussian, $a^\dagger |t\alpha\rangle$ or $a^\dagger |\varkappa\alpha\rangle$) with certain ration. Observing the forms of the SPCCSs ($|\alpha_c\rangle_{BS}$ and $|\alpha_c\rangle_{PA}$) in Eqs.(1) and (2), one can

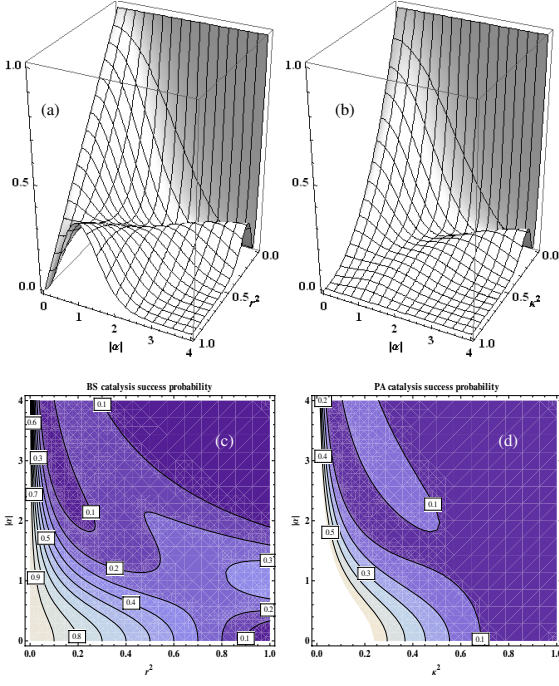


FIG. 2: (Color online) The success probabilities of detection (a) and (c) for p_{BS} as a function of interaction parameter $|\alpha|$ and r^2 ; (b) and (d) for p_{PA} as a function of interaction parameter $|\alpha|$ and κ^2 .

find that they are all the superposition states of a coherent state and a photon-added coherent state. A question on whether there exist a kind of link between $|\alpha_c\rangle_{BS}$ and $|\alpha_c\rangle_{PA}$ is naturally arisen? Here we will discuss this question.

Expanding $|\alpha_c\rangle_{BS}$ and $|\alpha_c\rangle_{PA}$ into the Fock basis, we have the same form as follows

$$|\alpha_c\rangle_\Lambda = \sum_{n=0}^{\infty} \omega_n^\Lambda |n\rangle, \quad (3)$$

with the coefficients

$$\omega_n^\Lambda = \frac{\alpha^n e^{-(1-\Lambda)|\alpha|^2/2}}{\sqrt{n! I_0(\alpha, \Lambda)}} \times \sqrt{1-\Lambda}^{n-1} (1-\Lambda-n\Lambda), \quad (4)$$

leading to the photon number distribution (PND) of the catalyzed states $P_\Lambda(n) = |\omega_n^\Lambda|^2$. It is found that $|\alpha_c\rangle_{BS}$ and $|\alpha_c\rangle_{PA}$ are the same quantum states as long as the condition $\Lambda = r^2 = \kappa^2$ is satisfied. Here is equate to r^2 for the BS case and κ^2 for the PA case. By analyzing the construction of the generated states, we verify that the SPCCS generated on the BS is equal to that generated on the PA if we choose the appropriate catalysis parameters.

It is obvious to see that the SPCCSs are characterized by two parameters, i.e. the input parameter α and the catalysis parameter Λ . By adjusting the parameters, the coefficients may be modulated, generating a wide range

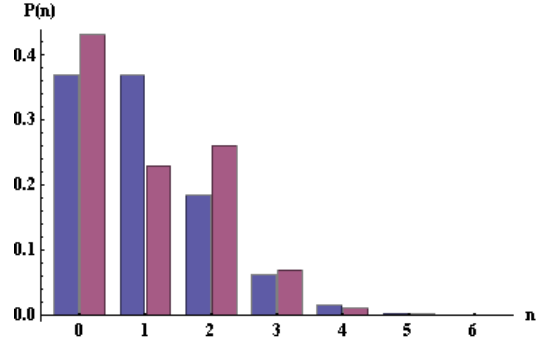


FIG. 3: (Color online) Photon-number distributions of (a) Coherent state $|\alpha\rangle$ with $|\alpha| = 1$ (blue bars) and (b) the SPCCS with $|\alpha| = 1$ and $\Lambda = r^2 = \kappa^2 = 0.7$ (purple bars).

of nonclassical phenomena, as seen in the Sec.IV. Especially, when $\Lambda = 0$, the SPCCS reduces to the input CS $|\alpha\rangle$ with $P_0(n) = e^{-|\alpha|^2} |\alpha|^{2n}/n!$ (Poissonian distribution) [20]; while $\Lambda = 1$, the SPCCS reduces to $|1\rangle$ with $P_1(n) = \delta_{1,n}$. In Fig.3 we plot the PNDs of the coherent state $|\alpha\rangle$ with $|\alpha| = 1$ and the SPCCS with $|\alpha| = 1$ and $\Lambda = 0.7$.

IV. NONCLASSICAL PROPERTIES OF THE SPCCS

Quantum states of light can be classified according to their statistical properties. They are usually compared to a reference state, namely, the coherent state [21]. Hence in this section, we compare the SPCCSs with the origin coherent state and discuss the nonclassical properties of the SPCCSs.

A. Sub-Poissonian distribution and anti-bunching effect

In this subsection, we examine the Mandel Q factor [22]

$$Q = \frac{\langle a^{\dagger 2} a^2 \rangle}{\langle a^\dagger a \rangle^2} - \langle a^\dagger a \rangle \quad (5)$$

and measure the second-order autocorrelation function [23]

$$g^{(2)}(0) = \frac{\langle a^{\dagger 2} a^2 \rangle}{\langle a^\dagger a \rangle^2}. \quad (6)$$

The distribution is Poissonian when $Q = 0$, and super-(sub-) Poissonian if $Q > 0$ ($Q < 0$), while the effect is antibunching when $g^{(2)}(0) < 1$ (strictly nonclassical), and bunching (superbunching) if $1 \leq g^{(2)}(0) \leq 2$ ($g^{(2)}(0) > 2$). For a coherent state, $g^{(2)}(0) = 1$ corresponds to $Q = 0$ (Poissonian statistics).

The variations of Q are depicted in Fig.4. Mandel Q factor as a function of for $|\alpha| = 1, 2, 3$ is plotted in

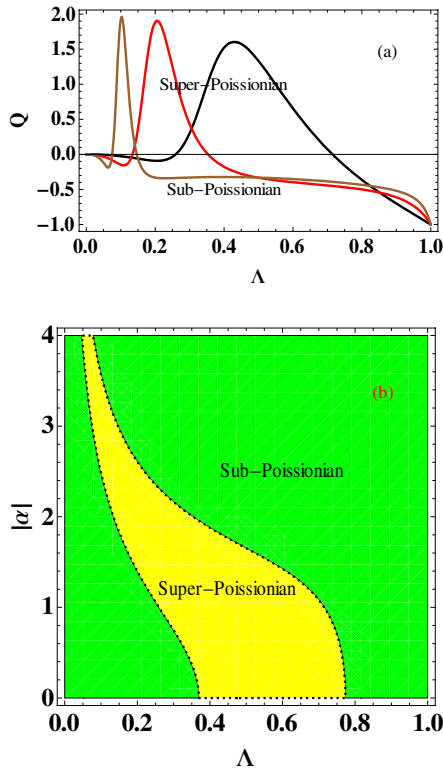


FIG. 4: (Color online) (a) Mandel Q parameter as a function of the catalysis parameter Λ for different $|\alpha|$, where the black, red, and brown lines are corresponding to $|\alpha| = 1$, $|\alpha| = 2$, and $|\alpha| = 3$, respectively. (b) The feasibility regions in $(\Lambda, |\alpha|)$ space showing sub-Poissonian distribution $Q < 0$ (strictly nonclassical), and -Poissonian distribution $Q > 0$.

Fig.4(a). The feasibility regions of super-Poisson and sub-Poisson distribution are shown in Fig.4(b). For $\Lambda \rightarrow 0$, Q approaches the values for a coherent state, i.e. $Q = 0$; while $\Lambda \rightarrow 1$, Q approaches the values for a single-photon Fock state, i.e. $Q = -1$. Similarly, the second-order autocorrelation function as a function of for $|\alpha| = 1, 2, 3$ is plotted in Fig.5(a) and the feasibility regions of antibunching, bunching and superbunching are shown in Fig.5(b). For $\Lambda \rightarrow 0$, $g^{(2)}(0)$ approaches the values for a coherent state, i.e. $g^{(2)}(0) = 1$; while $\Lambda \rightarrow 1$, $g^{(2)}(0)$ approaches the values for a single-photon Fock state, i.e. $g^{(2)}(0) = 0$. It is found that there may present sub-Poissonian and antibunching effect in a wide range of interaction parameters for the SPCCSs. In the limiting case, when $\Lambda = 0$, the states corresponding to CS $|\alpha\rangle$, then $Q = 0$ and $g^{(2)}(0) = 1$; while for $\Lambda = 1$, the states corresponding to single-photon Fock state $|1\rangle$, then $Q = -1$ and $g^{(2)}(0) = 0$.

B. Quadrature squeezing effect

Next, we explore another nonclassical effect, i.e., squeezing of quadrature amplitude, which is defined

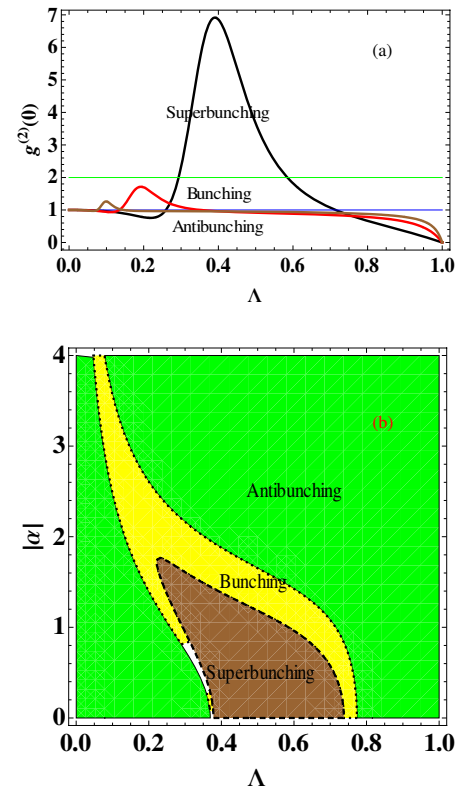


FIG. 5: (Color online) (a) Second-order autocorrelation function $g^{(2)}(0)$ as a function of the catalysis parameter Λ for different $|\alpha|$, where the black, red, and brown lines are corresponding to $|\alpha| = 1$, $|\alpha| = 2$, and $|\alpha| = 3$, respectively. (b) The feasibility regions in $(\Lambda, |\alpha|)$ space showing antibunching $g^{(2)}(0) < 1$ (strictly nonclassical), bunching $1 \leq g^{(2)}(0) \leq 2$, and superbunching $g^{(2)}(0) > 2$.

from two quadrature operators $X = (a + a^\dagger)/\sqrt{2}$ and $P = (a - a^\dagger)/(\sqrt{2}i)$. Both quadrature variances can be expressed as

$$\begin{aligned} \langle \Delta X^2 \rangle &= \langle a^\dagger a \rangle - \langle a^\dagger \rangle \langle a \rangle + \frac{1}{2} \\ &+ \frac{\langle a^{\dagger 2} \rangle - \langle a^\dagger \rangle^2}{2} + \frac{\langle a^2 \rangle - \langle a \rangle^2}{2}, \end{aligned} \quad (7)$$

and

$$\begin{aligned} \langle \Delta P^2 \rangle &= \langle a^\dagger a \rangle - \langle a^\dagger \rangle \langle a \rangle + \frac{1}{2} \\ &- \frac{\langle a^{\dagger 2} \rangle - \langle a^\dagger \rangle^2}{2} - \frac{\langle a^2 \rangle - \langle a \rangle^2}{2}, \end{aligned} \quad (8)$$

respectively, as can be seen from their definitions [24]. The uncertainty relation obeys $\Delta X^2 \Delta P^2 \geq 1/4$. For a coherent (vacuum) state, the variances of X and P are equal to $1/2$. If one of ΔX^2 and ΔP^2 is smaller than $1/2$, then this state is squeezing. Moreover, one can also adopt quantum squeezing quantified in a dB scale through $dB[X] = 10 \log_{10} (\Delta X^2 / \Delta X^2|_{|0\rangle})$, $dB[P] =$

$10 \log_{10} (\Delta P^2 / \Delta P^2|_{|0\rangle})$, i.e., these quadrature variances, relative to their vacuum values of $\Delta X^2|_{|0\rangle} = \Delta P^2|_{|0\rangle} = 1/2$. Hence, if one of $dB[X]$ and $dB[P]$ is less than 0, this quantum is squeezed state.

In Fig.6(a) we plot the variation of $dB[X]$ as a function of the catalysis parameter Λ for different $|\alpha|$. It is clearly seen that for a given $|\alpha|$ there exists squeezing in X quadrature component in some range of catalysis parameter Λ . The maximum and minimum variances can be found by using the scientific computing software MATHEMATICA. For the case of $|\alpha| = 1$ (see the black line in Fig.7 (a)), the largest squeezing (corresponding the minimum variance $\Delta X^2 = 3/8$) is attainable at $\Lambda = 0.322185$, below the vacuum noise level of $1/2$ by 1.25dB. The maximum variance of $3/2$ corresponds to 4.77dB antisqueezing at $\Lambda = 1$. For the case of $|\alpha| = 2$ (see the red line in Fig.7 (b)), the largest squeezing (corresponding the minimum variance $\Delta X^2 = 3/8$) is attainable at $\Lambda = 0.129649$, below the vacuum noise level of $1/2$ by 1.25dB. The maximum variance of $3/2$ corresponds to 4.77dB antisqueezing at $\Lambda = 0.25$ and $\Lambda = 1$. For the case of $|\alpha| = 3$ (see the brown line in Fig.7 (c)), the largest squeezing (corresponding the minimum variance $\Delta X^2 = 3/8$) is attainable at $\Lambda = 0.0695085$, below the vacuum noise level of $1/2$ by 1.25dB. The maximum variance of $3/2$ corresponds to 4.77dB antisqueezing at $\Lambda = 0.111111$ and $\Lambda = 1$. In Fig.6(b), we plot the contour of $dB[X]$ in $(\Lambda, |\alpha|)$ plain parameter space. The regions with $dB[X] < 0$ show the squeezing effect. In the limiting case, when $\Lambda = 0$, the states corresponding to CS $|\alpha\rangle$, then $dB[X] = 0dB$; while for $\Lambda = 1$, the states corresponding to single-photon Fock state $|1\rangle$, then $dB[X] = 4.77dB$.

V. WIGNER FUNCTION OF THE SPCCS

The negative Wigner function is a witness of the non-classicality of a quantum state [25]. In this section, we derive the analytical expression of the WF and make numerical analysis for the character of the SPCCSs. For a single-mode density operator ρ , the WF in the coherent state representation $|z\rangle$ can be expressed as $W(\beta) = \frac{2e^{2|\beta|^2}}{\pi} \int \frac{d^2z}{\pi} \langle -z|\rho|z\rangle e^{-2(z\beta^* - z^*\beta)}$, where $\beta = (q + ip)/\sqrt{2}$ [26]. For the SPCCS, the WF is

$$W(\beta; \alpha, \Lambda) = \frac{2F(\beta; \alpha, \Lambda)}{\pi I_0(\alpha, \Lambda)} e^{-2|\beta - \sqrt{1-\Lambda}\alpha|^2}, \quad (9)$$

where the defined function is

$$\begin{aligned} F(\beta; \alpha, \Lambda) &= (1 - \Lambda) - \Lambda(3\Lambda - 2)|\alpha|^2 \\ &+ \Lambda^2(1 - \Lambda)|\alpha|^4 + 4\Lambda^2|\alpha|^2|\beta|^2 \\ &- 2\Lambda\sqrt{1 - \Lambda} \left(1 + \Lambda|\alpha|^2\right) (\alpha\beta^* + \beta\alpha^*). \end{aligned} \quad (10)$$

Obviously, the WF $W(\beta; \alpha, \Lambda)$ in Eq.(9) is non-Gaussian in the phase space due to the presence of the term

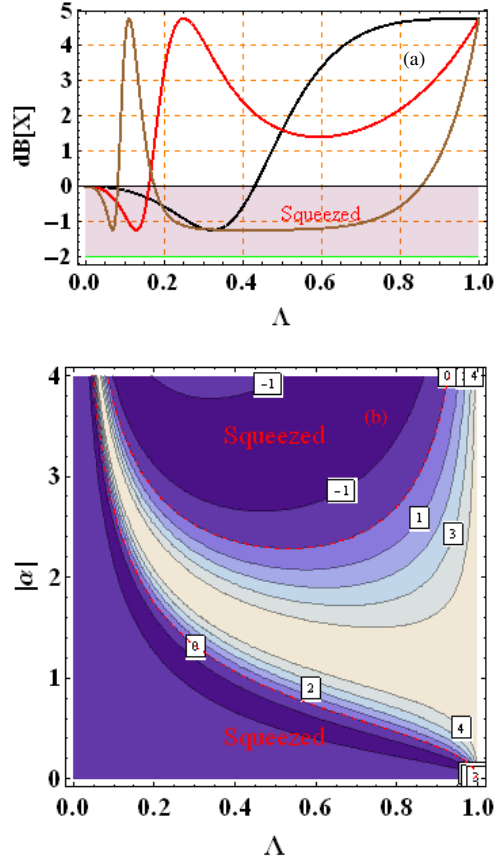


FIG. 6: (Color online) (a) Quadrature variance of the X component, relative to the vacuum (unsqueezed) state in units of dB, as a function of the catalysis parameter Λ for different $|\alpha|$, where the black, red, and brown lines are corresponding to $|\alpha| = 1$, $|\alpha| = 2$, and $|\alpha| = 3$, respectively. The grey region shows squeezed. (b) The contourplot of $dB[X]$ in the $(\Lambda, |\alpha|)$ parameter plain space, where squeezing regions correspond the condition of $dB[X] < 0$.

$F(\beta; \alpha, \Lambda)/I_0(\alpha, \Lambda)$. In addition, it indicates that if $F(\beta; \alpha, \Lambda) < 0$ then there is negative region in phase space. In particular, when $\Lambda = 0$, Eq.(9) just reduces to the WF of the CS $|\alpha\rangle$, i.e., $W(\beta; \alpha, 0) = \frac{2}{\pi} e^{-2|\beta - \alpha|^2}$; when $\Lambda = 1$, Eq.(6) just reduces to the WF of single-photon Fock state $|1\rangle$, i.e., $W(\beta; \alpha, 1) = \frac{2}{\pi} (4|\beta|^2 - 1) e^{-2|\beta|^2}$. The Wigner distributions for several SPCCSs with $\alpha = 1 + i$, $\alpha = 2$, and $\alpha = 2.7$ are depicted in phase space in Fig.7. There exist some obvious negative regions in the phase space, which is an important figure of merit for a non-Gaussian quantum state.

On the other hand, the negative volume of the WF defined by

$$\delta = \frac{1}{2} \left[\int_{-\infty}^{\infty} \int_{-\infty}^{\infty} dqdp |W(q, p)| - 1 \right]. \quad (11)$$

is a good indicator of non-classicality for a quantum state [27]. In Fig.8, we plot the negative volume δ of WF as a function of different catalysis parameter Λ for several

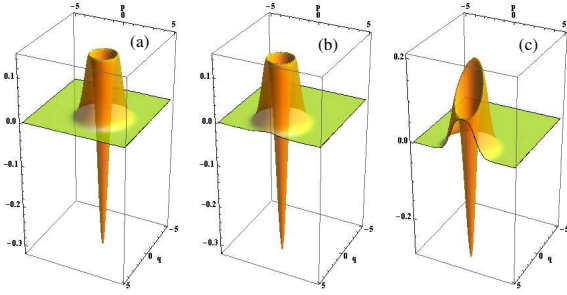


FIG. 7: (Color online) Wigner functions of the SPCCSs for some different parameters with (a) $\alpha = 1 + i$, $\Lambda = 0.5$; (b) $\alpha = 2$, $\Lambda = 0.25$; and (c) $\alpha = 2.7$, $\Lambda = 0.125$. Outstanding characteristic is the negativity of the Wigner functions.

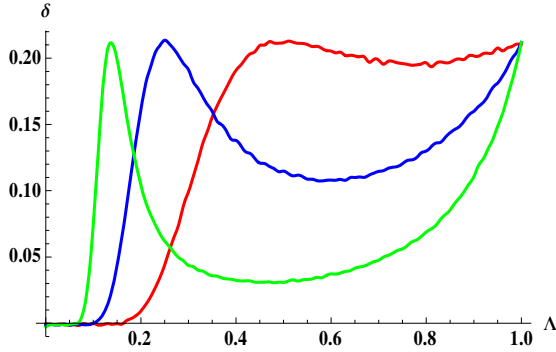


FIG. 8: (Color online) Negative volume of Wigner functions δ of the SPCCSs as a function of the catalysis parameter Λ for different input coherent state $|\alpha\rangle$ with $\alpha = 1 + i$ (red line), $\alpha = 2$ (blue line) and $\alpha = 2.7$ (green line).

SPCCSs with $\alpha = 1 + i$, $\alpha = 2$, and $\alpha = 2.7$. In addition, the negative areas are modulated not only by the input parameter α , but also by the catalysis parameter Λ . It is found that for every given input $|\alpha\rangle$, there exist a maximum volume δ_{\max} in a moderate catalysis parameter Λ . For instance, δ_{\max} is found at around $\Lambda = 0.5$ for $\alpha = 1 + i$, at around $\Lambda = 0.25$ for $\alpha = 2$, and at around $\Lambda = 0.125$ for $\alpha = 2.7$. Hence by adjusting the catalysis parameter Λ , the optimal nonclassicality (i.e. δ_{\max}) can be obtained for a given input coherent state $|\alpha\rangle$. In addition, we also show that two extreme cases, i.e., $\delta_{|\alpha\rangle} = 0$ for $\Lambda = 0$ and $\delta_{|1\rangle} = 0.211081$ for $\Lambda = 1$, are always right, as expected.

VI. CONCLUSION

In summary, we have proved the equivalent effect between the lossless beam splitter and the nondegenerate parametric amplifier in quantum state engineering. We report theoretical preparation and nonclassical properties of a kind of new non-Gaussian quantum states, i.e. single-photon catalyzed coherent states (SPCCSs). These states are generated by operating single-photon

quantum-optical catalysis on a coherent state. Lossless beam splitter and nondegenerate parametric amplifier are used as the catalyzed devices respectively. We prove that the catalyzed coherent states are actually the same quantum states. Although the success probabilities of the detection are different, the effects of BS and PA are equivalent once the detections are succeed. The quantum properties of the catalyzed states, such as photon number distribution, quadrature squeezing effect, Mandel Q parameter, autocorrelation function and Wigner function are investigated. Simple extensions of the catalysis scheme allow for the preparation of more sophisticated quantum states.

Acknowledgments

This work was supported by the National Nature Science Foundation of China (Grants No. 11264018 and No. 11447002) and the Natural Science Foundation of Jiangxi Province of China (Grants No. 20142BAB202001 and No. 20151BAB202013)

Appendix A: Character of the SPCCS generated by BS

We give the detailed procedure of derivating the explicit form of the SPCCS $|\alpha_c\rangle_{BS}$ by BS. Noting the coherent state $|\alpha_a\rangle = e^{-|\alpha|^2/2} e^{\alpha a^\dagger} |0_a\rangle$ and the Fock state $|1_b\rangle = \frac{d}{ds_1} e^{s_1 b^\dagger} |0_b\rangle|_{s_1=0}$, we rewrite $|\alpha_c\rangle_{BS}$ as

$$\begin{aligned} |\alpha_c\rangle_{BS} &= \frac{e^{-|\alpha|^2/2}}{\sqrt{p_{BS}}} \frac{d^2}{dt_1 ds_1} e^{(\alpha t + s_1 r) a^\dagger} |0_a\rangle \\ &\quad \times \langle 0_b | e^{t_1 b} e^{(s_1 t - \alpha r) b^\dagger} |0_b\rangle|_{s_1=t_1=0}, \\ &= \frac{e^{-|\alpha|^2/2}}{\sqrt{p_{BS}}} \frac{d^2}{dt_1 ds_1} e^{ts_1 t_1 - r\alpha t_1 + a^\dagger t \alpha + a^\dagger r s_1} |0_a\rangle|_{s_1=t_1=0} \\ &= \frac{e^{-|\alpha|^2/2}}{\sqrt{p_{BS}}} (t - a^\dagger r^2 \alpha) \exp(t \alpha a^\dagger) |0_a\rangle. \end{aligned}$$

Thus the explicit form in Eq.(1) is obtained. In addition, its density operator can be read as

$$\begin{aligned} \rho_{c-B} &= \frac{e^{-|\alpha|^2}}{p_{BS}} \frac{d^4}{dt_1 ds_1 dt_2 ds_2} e^{ts_1 t_1 - r\alpha t_1 + ts_2 t_2 - r\alpha^* t_2} \\ &\quad \times e^{a^\dagger t \alpha + a^\dagger r s_1} |0_a\rangle \langle 0_a | e^{at \alpha^* + ar s_2} |_{s_1=t_1=s_2=t_2=0}, \end{aligned}$$

and then its success probability p_{BS} is obtained

$$\begin{aligned} p_{BS} &= e^{-|\alpha|^2} \frac{d^4}{dt_1 ds_1 dt_2 ds_2} e^{ts_1 t_1 - r\alpha t_1 + ts_2 t_2 - r\alpha^* t_2} \\ &\quad \times e^{r^2 s_1 s_2 + t^2 \alpha \alpha^* + r t \alpha s_2 + r t s_1 \alpha^*} |_{s_1=t_1=s_2=t_2=0}. \end{aligned}$$

Appendix B: Character of the SPCCS generated by PA

We give the detailed procedure of derivating the explicit form of the SPCCS $|\alpha_c\rangle_{PA}$ by PA. Noting the integration of squeezing operator $S(\lambda) = \int \frac{d^2 \eta}{\mu \pi} \left| \frac{\eta}{\mu} \right\rangle \langle \eta |$ (with

$\mu = e^\lambda$ and $|\eta\rangle = e^{-\frac{|\eta|^2}{2} + \eta a^\dagger - \eta^* b^\dagger + a^\dagger b^\dagger} |0_a, 0_b\rangle$ and the Fock state $|1_b\rangle = \frac{d}{ds_1} e^{s_1 b^\dagger} |0_b\rangle|_{s_1=0}$, we rewrite $|\alpha_c\rangle_{PA}$ as

$$\begin{aligned} & |\alpha_c\rangle_{PA} \\ &= \frac{1}{\sqrt{p_{PA}}} \frac{d^2}{ds_1 dt_1} \\ & \times \int \frac{d^2 \eta}{\mu \pi} \langle 0_b | e^{t_1 b} e^{-\frac{|\eta|^2}{2} + \frac{\eta}{\mu} a^\dagger - \frac{\eta^*}{\mu} b^\dagger + a^\dagger b^\dagger} |0_a, 0_b\rangle \\ & \times \langle 0_a, 0_b | e^{-\frac{|\eta|^2}{2} + \eta^* a - \eta b + ab} |\alpha_a\rangle e^{s_1 b^\dagger} |0_b\rangle |_{s_1=t_1=0} \\ &= \frac{\varkappa e^{-|\alpha|^2/2}}{\sqrt{p_{PA}}} \frac{d^2}{ds_1 dt_1} e^{-\kappa \alpha s_1 + \varkappa s_1 t_1 + \kappa t_1 a^\dagger + \varkappa \alpha a^\dagger} |0_a\rangle |_{s_1=t_1=0} \\ &= \frac{\varkappa e^{-|\alpha|^2/2}}{\sqrt{p_{PA}}} (\varkappa - \alpha a^\dagger \kappa^2) e^{\varkappa \alpha a^\dagger} |0_a\rangle. \end{aligned}$$

Thus the explicit form in Eq.(2) is obtained. Meanwhile, its density operator can be read as

$$\begin{aligned} \rho_{c-PA} &= \frac{\varkappa^2 e^{-|\alpha|^2}}{p_{PA}} \frac{d^4}{ds_1 dt_1 ds_2 dt_2} \\ & \times e^{-\kappa \alpha s_1 + \varkappa s_1 t_1 - \kappa \alpha^* s_2 + \varkappa s_2 t_2} \\ & \times e^{(\kappa t_1 + \varkappa \alpha) a^\dagger} |0\rangle \langle 0| e^{(\kappa t_2 + \varkappa \alpha^*) a} |_{s_1=t_1=s_2=t_2=0}, \end{aligned}$$

and then its success probability p_{PA} is obtained

$$\begin{aligned} p_{PA} &= \varkappa^2 e^{-\kappa^2 |\alpha|^2} \frac{d^4}{ds_1 dt_1 ds_2 dt_2} e^{\varkappa(s_1 t_1 + s_2 t_2) + t_1 t_2 \kappa^2} \\ & \times e^{(\varkappa t_2 - s_1) \alpha \kappa + (\varkappa t_1 - s_2) \alpha^* \kappa} |_{s_1=t_1=s_2=t_2=0}. \end{aligned}$$

Appendix C: Statistical quantities of the SPCCS

In order to explore the statistical quantities of the SPCCS, we give the general form of expectation value $\langle a^{\dagger k} a^l \rangle$ as follows

$$\begin{aligned} & \langle a^{\dagger k} a^l \rangle_{BS} \\ &= \frac{e^{-r^2 |\alpha|^2}}{p_{BS}} \frac{d^{4+k+l}}{dt_1 ds_1 dt_2 ds_2 d\mu^k d\nu^l} \\ & \times e^{ts_2 t_2 - r \alpha^* t_2 + t s_1 t_1 - r \alpha t_1 + t \alpha \nu + r \nu s_1 + r^2 s_1 s_2 + r \mu s_2} \\ & \times e^{+t \mu \alpha^* + r t \alpha s_2 + r t s_1 \alpha^*} |_{s_1=t_1=s_2=t_2=\mu=\nu=0}, \end{aligned}$$

and

$$\begin{aligned} & \langle a^{\dagger k} a^l \rangle_{PA} \\ &= \frac{\varkappa^2 e^{-\kappa^2 |\alpha|^2}}{p_{PA}} \frac{d^{4+k+l}}{dt_1 ds_1 dt_2 ds_2 d\mu^k d\nu^l} \\ & \times e^{(\nu \alpha + \mu \alpha^*) \varkappa + (s_1 t_1 + s_2 t_2) \varkappa - (s_1 \alpha + s_2 \alpha^*) \kappa + (t_2 \alpha + t_1 \alpha^*) \varkappa \kappa} \\ & \times e^{+(\mu t_2 + \nu t_1) \kappa + t_1 t_2 \kappa^2} |_{s_1=t_1=s_2=t_2=r_1=r_2=0}. \end{aligned}$$

where we remain their differential forms. For different k and l , we have

$$\begin{aligned} \langle a^\dagger \rangle_\Lambda &= \langle a \rangle_\Lambda^* = \frac{I_1(\alpha, \Lambda)}{I_0(\alpha, \Lambda)} \sqrt{(1-\Lambda)} \alpha^*, \\ \langle a^{\dagger 2} \rangle_\Lambda &= \langle a^2 \rangle_\Lambda^* = \frac{I_2(\alpha, \Lambda)}{I_0(\alpha, \Lambda)} (1-\Lambda) \alpha^{*2}, \\ \langle a^\dagger a \rangle_\Lambda &= \frac{I_3(\alpha, \Lambda)}{I_0(\alpha, \Lambda)} |\alpha|^2, \\ \langle a^{\dagger 2} a^2 \rangle_\Lambda &= \frac{I_4(\alpha, \Lambda)}{I_0(\alpha, \Lambda)} (1-\Lambda) |\alpha|^4, \end{aligned}$$

where the functions are defined as

$$\begin{aligned} I_0(\alpha, \Lambda) &= (1-\Lambda) + \Lambda(3\Lambda-2) |\alpha|^2 \\ & \quad + \Lambda^2 (1-\Lambda) |\alpha|^4, \\ I_1(\alpha, \Lambda) &= (1-2\Lambda) + 2\Lambda(2\Lambda-1) |\alpha|^2 \\ & \quad + \Lambda^2 (1-\Lambda) |\alpha|^4, \\ I_2(\alpha, \Lambda) &= (1-3\Lambda) + \Lambda(5\Lambda-2) |\alpha|^2 \\ & \quad + \Lambda^2 (1-\Lambda) |\alpha|^4, \\ I_3(\alpha, \Lambda) &= (2\Lambda-1)^2 + \Lambda(1-\Lambda)(5\Lambda-2) |\alpha|^2 \\ & \quad + \Lambda^2 (1-\Lambda)^2 |\alpha|^4, \\ I_4(\alpha, \Lambda) &= (3\Lambda-1)^2 + \Lambda(1-\Lambda)(7\Lambda-2) |\alpha|^2 \\ & \quad + \Lambda^2 (1-\Lambda)^2 |\alpha|^4. \end{aligned}$$

with $\Lambda = r^2$ for the BS catalysis and $\Lambda = \kappa^2$ for the PA catalysis.

-
- [1] J. von Neumann, *Mathematical Foundations of Quantum Mechanics* (Princeton University Press, Princeton, 1955).
[2] M. Dakna, L. Knoll, and D. Welsch, *Opt. Commun.* 145 (1998) 309.
[3] S. A. Podoshvedov, J. Kim, and J. Lee, *Opt. Commun.* 281 (2008) 3748.
[4] M. Dakna, T. Anhut, T. Opatrny, L. Knoll, and D. G. Welsch, *Phys. Rev. A* 55 (1997) 3184.
[5] B. M. Escher, A. T. Avelar, and B. Baseria, *Phys. Rev. A* 72 (2005) 045803.
[6] J. Fiurasek, R. Garcia-Patron, and N. J. Cerf, *Phys. Rev. A* 72 (2005) 033822.
[7] M. Takeoka and M. Sasaki, *Phys. Rev. A* 75 (2007) 064302.
[8] J. Fiurasek, S. Massar, and N. J. Cerf, *Phys. Rev. A* 68 (2003) 042325.
[9] J. Laurat, T. Coudreau, N. Treps, A. Maitre, and C. Fabre, *Phys. Rev. A* 69 (2004) 033808.
[10] B. Yurke, S. L. McCall, and J. R. Klauder, *Phys. Rev. A* 33 (1986) 4033.
[11] M. Ban, *Phys. Lett. A* 233 (1997) 284.
[12] A. I. Lvovsky and J. Mlynek, *Phys. Rev. Lett.* 88 (2002) 250401.
[13] T. J. Bartley, G. Donati, J. B. Spring, X. M. Jin, M. Barbieri,

- A. Datta, B. J. Smith, and I. A. Walmsley, *Phys. Rev. A* 86 (2012) 043820.
- [14] X. X. Xu, *Phys. Rev. A* 92 (2015) 012318.
- [15] M. Ban, *Opt. Commun.* 143 (1997) 225.
- [16] S. M. Barnett and P. M. Radmore, *Methods in Theoretical Quantum Optics* (Clarendon Press, Oxford, 1997).
- [17] J. K. Asboth, J. Calsamiglia, and H. Ritsch, *Phys. Rev. Lett.* 94 (2005) 173602.
- [18] D. F. Walls and G. J. Miburn, *Quantum Optics* (Springer-Verlag Berlin Heidelberg, New York, 1994).
- [19] M. O. Scully and M. S. Zubairy, *Quantum Optics* (Cambridge Univ. Press 1997).
- [20] J. R. Klauder and B. Skagerstam, *Coherent States* (World Scientific, Singapore, 1985).
- [21] V. V. Dodonov and V. I. Man'ko, *Theory of nonclassical states of light* (Taylor & Francis Group, 2003).
- [22] L. Mandel, Sub-Poissonian photon statistics in resonance fluorescence, *Opt. Lett.* 4 (1979) 205.
- [23] L. Davidovich, Sub-Poissonian processes in quantum optics, *Rev. Mod. Phys.* 68 (1996) 127.
- [24] J. C. Garrison and R.Y. Chiao, *Quantum Optics* (Oxford University Press, New York, 2008)
- [25] R. Filip, *Phys. Rev. A* 87 (2013) 042308.
- [26] K. E. Cahill and R. J. Glauber, *Phys. Rev.* 177 (1969) 1882.
- [27] A. Kenfack and K. Zyczkowski, *J. Opt. B: Quantum Semi-class. Opt.* 6 (2004) 396.